Proceedings of IMECE2005
2005 ASME International Mechanical Engineering Congress and Exposition
November 5-11, 2005, Orlando, Florida USA

IMECE2005-81912

THERMODYNAMIC ANALYSIS OF PRODUCTION OF HYDROGEN USING HIGH-TEMPERATURE FUEL CELLS

Elisângela Martins Leal
Mechanical and Aerospace Engineering Department
University of California, Irvine CA 92697
eleal@uci.edu

Jacob Brouwer
National Fuel Cell Research Center
University of California, Irvine CA 92697
jb@nfcrc.uci.edu

ABSTRACT

This paper presents: (1) the electricity and hydrogen co-production concept, (2) a thermodynamic analysis methodology for studying solid oxide and molten carbonate fuel cell hydrogen co-production, and (3) simulation results that address the impact of reformer placement in the cycle on system performance. The methodology is based on detailed thermodynamic and electrochemical principles that apply to each of the system components and the integrated cycles. Eight different cycle configurations that use fuel cell heat to drive hydrogen production in a reformer are proposed, analyzed, and compared. The specific cycle configurations include SOFC and MCFC cycles using both external and internal reforming options. The fuel cell plant performance has been evaluated on the basis of methane utilization efficiency and each component of the plant has been evaluated on the basis of second law efficiency. The analyses show that in all cases the exergy losses (irreversibilities) in the combustion chamber are the most significant losses in the cycle. Furthermore, for the same power output, the internal reformation option has the higher electrical efficiency and produces more hydrogen per unit of fuel supplied, in the case of using a SOFC.

Keywords: Solid oxide fuel cell, molten carbonate fuel cell, steam reforming, hydrogen production, thermodynamic analysis.

INTRODUCTION

Interest in the hydrogen economy and in fuel cells has increased dramatically in recent years. The main reason is that a hydrogen economy may be an answer to the two major challenges facing the future global economy: climate change and the security of energy supplies. Both these challenges call for development of new, highly efficient technologies that are either carbon neutral or low emitting technologies. High-temperature fuel cells, such as molten carbonate (MCFC) and solid oxide fuel cells (SOFC), are promising for the conversion of a fuel chemical energy into electricity, attaining significantly higher efficiencies compared to similarly sized energy conversion devices, such as gas turbines and internal combustion engines. Furthermore, these kinds of fuel cells produce high-temperature waste heat that can be used for cogeneration, which in this particular case is used to produce hydrogen for other uses.

The main processes for hydrogen production are presented in several literature sources [1 – 4]. Hydrogen production types include hydrocarbon-based processes (e.g., steam reforming, partial oxidation, gasification, catalytic decomposition), non-hydrocarbon-based processes (e.g., electrolytic, thermo-chemical, photochemical, photo-electrochemical) and integrated processes that may use renewable, nuclear, or other energy inputs. Steam-methane reforming is an important and common industrial processes for hydrogen production. Steam reformation produces a hydrogen-rich gas that is typically on the order of 70-75% hydrogen on a dry basis, along with smaller amounts of methane (2-6%), carbon monoxide (7-10%), and carbon dioxide (6-14%) [5]. Typical hydrogen production plants purify the hydrogen rich stream after steam reformation through a pressure swing absorption (PSA) or other purifying device.

The hydrogen economy, and in particular the use of hydrogen as an energy carrier for transportation applications, will depend upon local consumer access to inexpensive and environmentally sensitive pure hydrogen product delivery. Since hydrogen is challenging to store with high energy density, transport, distribution and dispensing of hydrogen typically involves a significant energy and environmental impact. In addition, the infrastructure required for transport, distribution and dispensing is likely to be expensive and require several decades to introduce. Thus, attention must be paid to developing a means of providing hydrogen to consumers in an environmentally sensitive manner.

One environmentally sensitive means of addressing both local generation of power and the production and distribution of hydrogen is to co-produce hydrogen and electricity using a high temperature stationary fuel cell system. Internal reforming high

temperature fuel cells, such as solid oxide fuel cells and molten carbonate fuel cells, are developed technologies with a few commercial products available. These systems do not require hydrogen; they are instead directly fuelled by natural gas or renewable fuel such as landfill or digester gas. The natural gas is reformed either indirectly or directly in the anode compartment to produce hydrogen. Direct reformation results in both promoting hydrogen production and providing needed cooling to the fuel cell stack. Indirect reformation occurs in a separate but thermally integrated reactor. Significantly, these fuel cell systems do not electrochemically consume all the fuel that is supplied (a fundamental limitation) and they produce enough heat to reform much more than the amount of hydrogen they consume.

In the present work we present this novel concept and develop a set of integrated SOFC and MCFC cycle configurations to study the impact of reformer placement in the cycle on system performance. A comparison between eight specific cycle configurations is presented in terms of both the First Law and Second Law of Thermodynamics analyses. The fuel cell heat is used to drive hydrogen production in an endothermic reformer using both external and internal reforming strategies.

We hypothesize that the local co-production of hydrogen and electricity will produce advantages compared to traditional hydrogen production strategies (e.g., steam reformation) in three ways: (1) production will be at the point of use averting emissions and energy impacts of hydrogen transport, (2) the use of fuel cell waste heat and steam as the primary inputs for the endothermic reforming process will use less fuel, and (3) a synergistic impact of lower fuel utilization on fuel cell voltage that can be exploited to increase fuel cell electrical efficiency. One potential disadvantage of this concept is incompatibility with future CO_2 sequestration options that are likely to be available only in certain locations.

NOMENCLATURE

a_{lk}	Number of atoms of element l in species k in the products [kmol]
b_l^0	Number of atoms of element l in the reactants [kmol]
Cp	Specific heat at constant pressure [kJ/kmol K]
E_0	Ideal standard potential [V]
E_{act}	Activation energy [J mol^{-1}]
E_F	Thermal energy of the fuel [kW]
Ex_{CH}	Chemical exergy [kW]
Ex_P	Exergy supplied by the recovered heat [kW]
Ex_S	Exergy supplied by the fuel [kW]
Ex_{TM}	Thermomechanical exergy [kW]
Ex_{TOT}	Total exergy [kW]
F	Faraday's constant [96,487 kC/kmol]
g	Molar Gibbs free energy [kJ/kmol]
ΔH_R	Net enthalpy change in the reaction [kJ]
h	Enthalpy [kJ/kmol]
h_k^f	Formation enthalpy per mole of species k at standard temperature and pressure [kJ/kmol]
j	Current density [A/m^2]
j_0	Exchange current density [A/m^2]
j_L	Limiting current density [A/m^2]
N	Molar flow [kmol/s]
n_e	Number of electrons participating in the reaction [mol e^-/mol]
P	Total pressure [MPa]
p_k	Partial pressure of the element k [MPa]
Q_{cv}	Heat in a control volume [kW]
Q_P	Recovered heat [kW]
R_{int}	Internal resistance [Ω]
R_{ohm}	Ohmic resistance [Ω]
R_u	Universal gas constant [8.314 kJ/kmol K]
S	Steam-to-carbon ration [-]
s	Entropy [kJ/kmol K]
S_{cv}	Entropy production in a control volume [kW/K]
T	Temperature [K]
V	Cell voltage [V]
W_{cv}	Work in a control volume [kW]
x	Coefficient that defines the carbon content of a fuel
y	Coefficient that defines the hydrogen content of a fuel

Subscripts and Superscrits:

0	At standard temperature and pressure
f	Formation
g	Gas
k	Species
l	Liquid
l	Species
P	Products
R	Reaction or Reactants

Greek letters:

α	Transfer coefficient
δ	Equivalent thickness of diffusion layer [m]
η_{act}	Activation polarization [V]
η_{conc}	Concentration polarization [V]
η_{an}	Impedance for anode overpotential [Ω]
η_{cat}	Impedance for cathode overpotential [Ω]
ε_{el}	Electrical efficiency
ε_F	Fuel efficiency or First Law efficiency
ε_{II}	Second Law efficiency
μ_k	Molar chemical potential of species k [kJ/kmol]
λ_l	Lagrange multiplier
η_{ohm}	Ohmic polarization [V]
ε_Q	Thermal efficiency

HIGH-TEMPERATURE FUEL CELLS

Molten Carbonate Fuel Cell

Among the various fuel cell types the molten carbonate fuel cell (MCFC) is emerging to become one of the principal, commercially available stationary power fuel cell system types. MCFC technology is well suited for stationary generation of electrical energy together with the production of relatively high quality heat fueled by natural gas. MCFC technology is thus suitable for many industrial applications as well as for distributed power supply. Molten carbonate fuel cells normally operate at a pressure between 1 and 10 bar and at a temperature of approximately 650°C. This operating temperature is needed to achieve sufficient conductivity in the carbonate electrolyte and is also advantageous for the system in several ways. First, high quality waste heat can be produced. Second, fuel flexibility is promoted through high temperature operation and an oxidizing ion to allow oxidation of carbon monoxide and light hydrocarbons in the anode compartment. Third, the high

temperature enables the use of lower cost metal cell components, since, for example, noble metal catalysts are not required to promote the electrochemical oxidation and reduction processes.

The carbonate fuel cell consists of two porous electrodes separated by a molten carbonate electrolyte (mixture of lithium and potassium salts), which serves to conduct carbonate ions from the cathode (the oxidant reducing electrode) to the anode (the fuel oxidizing electrode). The fuel cell operation is comprised of a complex combination of physical, chemical and electrochemical processes that work together to produce an external flow of electrons (the desired electrical work) by electrochemical oxidation of the fuel. The anodic, and cathodic half reactions are, respectively [6]:

$$H_2 + CO_3^{2-} \leftrightarrow H_2O + CO_2 + 2e^- \quad (1)$$

$$0.5\,O_2 + CO_2 + 2e^- \leftrightarrow CO_3^{2-} \quad (2)$$

Solid Oxide Fuel Cell

SOFC technology is promising for use in power generation applications, attaining significantly higher efficiencies compared to similarly sized energy conversion devices, such as gas turbines and internal combustion engines, when operated on natural gas. Furthermore, SOFC systems also produce high-temperature waste heat that can be used for cogeneration.

Independent of the fuel used in a SOFC system with an oxygen-ion-conducting electrolyte (the most common today), its operating principle relies on the continuous supply of fuel, containing H_2, CO, and CH_4 or other hydrocarbons, to the anode compartment while the cathode is supplied with air. The cathode half reaction for an SOFC is [7]:

$$0.5\,O_2 + 2e^- \rightarrow O^{2-} \quad (3)$$

The oxide ion is transported from cathode to anode through the yttria-stabilized zirconia electrolyte. At the anode, the oxide ions are consumed by the electrochemical oxidation of hydrogen to form steam releasing electrons to the external circuit [7]:

$$H_2 + O^{2-} \rightarrow H_2O + 2e^- \quad (4)$$

Like MCFC technology, high operating temperature leads to various advantages for SOFC operation on various fuel types, high quality waste heat, and no need for expensive electro-catalysts. This is especially true for an SOFC system that uses an appropriate external fuel processing technique, such as steam reforming, to produce a gas mixture that is rich in hydrogen. The electrochemically active species in SOFCs are H_2, CO, and hydrocarbons such as CH_4, but it is common in system-analysis practice to assume that only H_2 contributes to power generation while CH_4 is consumed through in-situ steam reforming, providing additional amounts of H_2 and CO and, CO is consumed through in situ water-gas-shift reactions, providing additional amounts of H_2 [8]. This assumption is reasonable due to both the hydrogen contribution that CO and the hydrocarbons make to the anode compartment, as well as the fact that hydrogen has substantially faster electrochemical kinetics compared to CO or hydrocarbons.

THERMODYNAMIC ANALYSES METHODS

Steam Reforming

A very common method of hydrogen production is the steam reforming process. Methane steam reforming consists of the reaction of methane and steam over a supported nickel catalyst at around 700ºC - 800°C to produce a mixture of H_2, CO, CO_2 and CH_4.

First, a global reaction mechanism is required to analyze the thermodynamics of steam reforming of a hydrocarbon fuel at a basic level [9]:

$$C_xH_y + Sx\,H_2O \leftrightarrow x\,CO_2 + (2x + 0.5\,y)H_2 + (S - 2)x\,H_2O \quad (5)$$

The term "global reaction" recognizes that the above reaction is actually the net result of a series of elementary reactions, some of which include catalytic interactions with surfaces. These are of no consequence to the overall thermodynamic analyses, but they are important to understand for reactor design and efficient operation and control of reformer systems. The overall balance of Eq. (5) conserves elements with two assumptions: there is sufficient steam to react with the fuel ($S \geq 2$), and the reaction goes to completion. Using Eq. (5), the formation enthalpies of the species can be added to determine the net enthalpy change as follows [9]:

$$\Delta H_R = x\,h^f_{CO_2} + (S-2)x\,h^f_{H_2O_{(g)}} - \left[h^f_{C_xH_y} + Sx\,h^f_{H_2O_{(l)}}\right] \quad (6)$$

Table 1 shows the net enthalpy change using a steam-to-carbon ratio equal to 2 and 3 for some hydrocarbon fuels.

TABLE 1. Net enthalpy change for some hydrocarbon fuels.

Comp.	x	y	h^f_{fuel} [kJ/kmol]	S	ΔH_R * [kJ/kmol]	S	ΔH_R * [kJ/kmol]
CH_4	1	4	-74,870	2	253,020	3	297,024
C_2H_6	2	6	-83,800	2	440,100	3	528,108
C_3H_8	3	8	-104,700	2	639,150	3	771,162
C_4H_{10}	4	10	-125,600	2	838,200	3	1,014,216
C_5H_{12}	5	12	-146,800	2	1,037,550	3	1,257,570
C_6H_{14}	6	14	-167,200	2	1,236,100	3	1,500,124
C_7H_{16}	7	16	-224,400	2	1,471,450	3	1,779,478

* The positive value means the process is endothermic.

Chemical Equilibrium Analysis

There are two common methods used to express chemical equilibrium. One method is based on the use of equilibrium constants, while the other is based on minimization of the free energy. One of the disadvantages of using equilibrium constants is that it is more difficult to test for the presence of condensed species in the reaction products. However, it is anticipated that solid carbon may be produced during the fuel reforming process, which can deactivate the catalytic reactions. Therefore, a method based on minimization of free energy is normally used in fuel reforming analysis.

Summarizing, for a given temperature and pressure, the equations for species conservation, atoms conservation, and condensed species are, respectively [10]:

$$N = \sum_{k=1}^{m} N_k \qquad k = 1, \ldots, m \quad (7)$$

$$b_l^0 = \sum_{k=1}^{m} a_{lk} N_k = b_l \qquad l = 1, \ldots, l \tag{8}$$

$$\frac{\mu_k^0}{R_u T} + \sum_{l=1}^{t} \left(\frac{\lambda_l}{R_u T} \right) a_{lk} = 0 \qquad k = m+1, \ldots, n \tag{9}$$

Equations (7) to (9) form a set of n + 1 equations that can be simultaneously solved for the unknowns N_k, λ_l and N. The thermodynamic function is then solved by the Newton-Raphson method for the unknowns. Figure 1 shows an example for the solution of the chemical equilibrium equations for methane as a function of temperature. As can be seen in Fig. 1, the best temperature to run a reformer is between 700ºC and 800ºC, a temperature condition for which production of hydrogen is maximized.

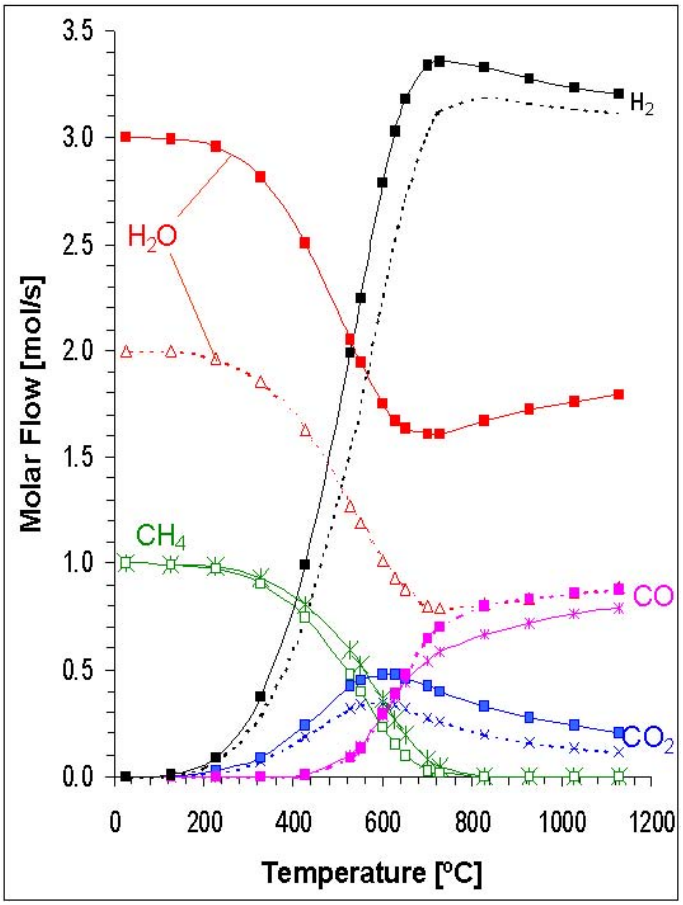

Figure 1. Results of production of hydrogen from methane as a function of temperature and steam-to-carbon ratio (solid line (S = 3) and dashed line (S = 2).

High-temperature fuel cells

Applying the steady flow energy equation and assuming negligible change of kinetic and potential energy, the First Law of Thermodynamics for a fuel cell system can be written as [11 – 14]:

$$\dot{Q}_{cv} - \dot{W}_{cv} + \sum_k (N_k h_k)_R - \sum_k (N_k h_k)_P = 0 \tag{10}$$

The molar enthalpy of each component (h_k) at a temperature T in a mixture of gases is calculated as [15]:

$$h_k = h_k^f + \int_{298\,K}^{T} Cp_k \, dT \tag{11}$$

Cp_k is the temperature-dependent specific heat capacity of component k. The entropy balance for the fuel cell system is given by [11, 12]:

$$\frac{\dot{Q}_{cv}}{T} - \sum_k (N_k s_k)_R - \sum_k (N_k s_k)_P + \dot{S}_{cv} = 0 \tag{12}$$

The entropy terms are correspondingly defined as [15]:

$$s_k = s_k^0 + \int_{298\,K}^{T} \frac{Cp_k}{T} dT - R_u \ln\left(\frac{p_k}{P^0} \right) \tag{13}$$

The Nernst equation for a MCFC and SOFC is given by [8, 9, 11 – 14]:

$$\text{MCFC:} \qquad E = E_0 + \frac{R_u T}{n_e F} \ln\left[\frac{p_{H_2} p_{O_2}^{0.5}}{p_{H_2O}} \cdot \frac{p_{CO_2,\text{cathode}}}{p_{CO_2,\text{anode}}} \right] \tag{14}$$

$$\text{SOFC} \qquad E = E_0 - \frac{R_u T}{n_e F} \ln\left[\frac{p_{H_2O} P}{p_{H_2} p_{O_2}^{0.5}} \right] \tag{15}$$

Voltage (V) can be calculated as [11 - 14]:

$$V = E - \eta_{act} - \eta_{conc} - \eta_{ohm} \tag{16}$$

$$\eta_{act} = \frac{R_u T}{\alpha n_e F} \ln\left[\frac{j}{j_0} \right] \tag{17}$$

$$\eta_{conc} = \frac{R_u T}{n_e F} \ln\left[1 - \frac{j}{j_L} \right] \tag{18}$$

$$\eta_{Ohm} = j R_{int} \tag{19}$$

Equations (17) to (19) are used to calculate the polarization losses in a fuel cell. They employ the Butler-Volmer equation to derive the equations for activation and concentration polarizations and Ohm's law for Ohmic polarization.

The total exergy of a flow consisting of many components (neglecting magnetic, electric and nuclear effects) is given by [19]:

$$Ex_{TOT} = Ex_{TM} + Ex_{CH} \tag{20}$$

The thermo-mechanical (Ex_{TM}) and chemical exergy (Ex_{CH}) can be written as, respectively [19]:

$$Ex_{TM} = \sum_{k=1}^{n} N_k (h_k - h_k^0) - T_0 \sum_{k=1}^{n} N_k (s_k - s_k^0) \tag{21}$$

$$Ex_{CH} = \sum_{k=1}^{n} x_k Ex_{ch,k}^0 + m R_u T_0 \sum_{k=1}^{n} x_k \ln x_k \tag{22}$$

Exergy analysis requires that the environment in which the system operates be well-defined. The temperature and pressure of the environment were set equal to the reference temperature and pressure (298K, 0.101 MPa) for all analyses in the current work. The atmosphere was modeled as an ideal-gas mixture with the composition shown in Table 2 [20].

Table 2 - Mole fractions and chemical exergy of the reference components in atmospheric air [20].

Component	Mole fraction	Chemical exergy (kJ/kmol)
N_2	0.7567	691.1
O_2	0.2035	3,946.7
H_2O	0.0303	8,667.9
CO_2	0.0003	20,108.5
Ar	0.0092	11,622.3

The fuel utilization efficiency is the ratio of all the useful energy extracted from the system (electrical and process heat) to the energy of the fuel input. Thus [19]:

$$\varepsilon_F = \varepsilon_{el} + \varepsilon_Q = \frac{W_{el} + Q_P}{E_F} \tag{23}$$

The second law efficiency is defined in the current analyses as the ratio of the amount of exergy in the products to the amount of exergy supplied in the reactants. This parameter is a more accurate measure of the thermodynamic performance of the system. Thus [19]:

$$\varepsilon_{II} = \frac{W_{el} + Ex_P}{Ex_S} \tag{24}$$

CYCLE CONFIGURATIONS

Solid oxide and molten carbonate fuel cell systems can be configured in many ways. Cycle configurations that include the potential for hydrogen co-production can be even more varied and complex. In the current paper we present several possible generic (and simple) cycle configurations that are considered for their potential electricity and hydrogen co-production capabilities. Then detailed thermodynamic and electrochemical analyses are accomplished on these eight specific cycle configurations, which use the high temperature fuel cell heat to drive hydrogen production in a reformer. Cycle configurations that consider both external and internal reforming options have been developed as shown in Figures 2, 3 and 4. Figure 2 shows the MCFC options: (a) the external reformer cycle configuration (config. 1), and (b) the internal reforming case (config. 2). Figures 3 and 4 show the SOFC options. Figure 3 shows the external reformer cycle configurations with the hydrogen production reformer placed in different positions in the cycle for each of the configurations 3-6. Figure 4 presents: (a) a different configuration for external reforming (with combustion chamber after the air pre-heater), and (b) the internal reforming case. These generic cycle configurations were developed to examine the general impacts of system design on the thermodynamic performance of high-temperature fuel cell cycles for hydrogen and electricity co-production. Each of the cycles contains pre-heaters for methane fuel preheat, air preheat, and water boiling and preheat. Each configuration also contains a reformer and a combustor. In all of the cases, the thermodynamic analyses use the equations presented above, which are comprised primarily of overall energy and exergy analyses.

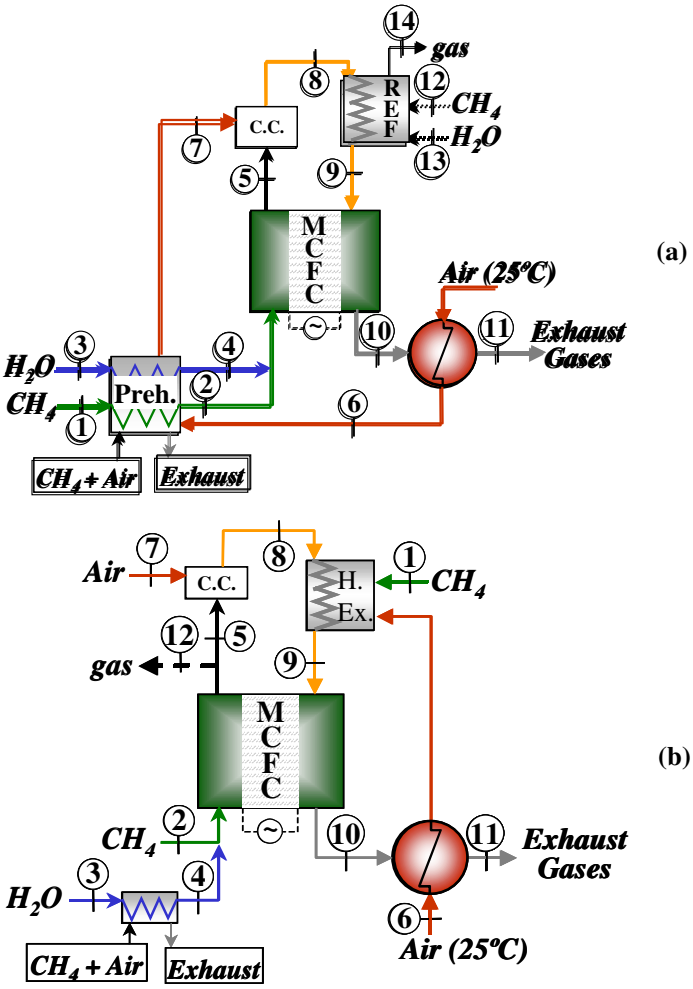

Figure 2. MCFC configurations: (a) External reforming (case 1), and (b) Internal reforming option (case 2).

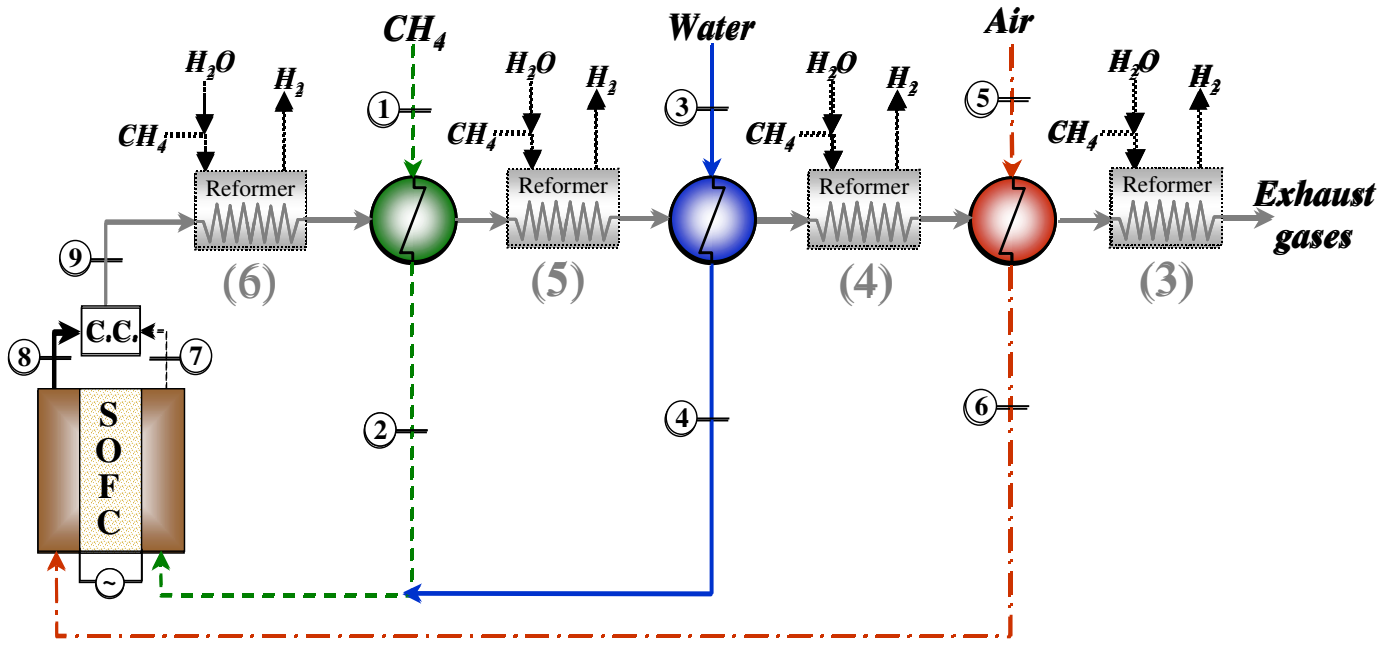

Figure 3. SOFC configurations 3 to 6: placement of a reformer in different locations (these configurations consist of the placement of a reformer: (3) after the air preheater, (4) after the water preheater, (5) after the methane preheater, and (6) after the combustion chamber).

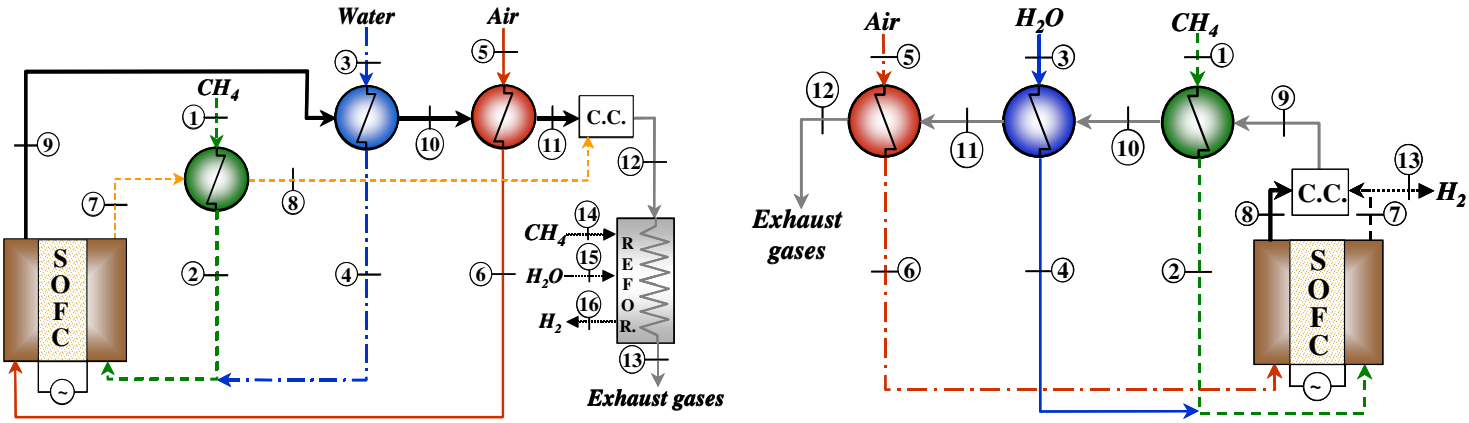

Figure 4. SOFC configurations 7 and 8: (a) External reforming with combustion chamber after the air preheater (7) and (b) Internal reforming option (8).

RESULTS AND DISCUSSION

The following considerations and assumptions are made for the analyses presented herein:

- Fuel cell electrical power output is 1,000 kW.
- Solid oxide fuel cell operating temperature is 1000ºC [8].
- Molten carbonate fuel cell operating temperature is 650ºC [22].
- Pre-heaters are 90% efficient and heat exchanger is 85% efficient [23].
- Fuel utilization in the anode compartment and oxidant utilization in the cathode compartment are fixed at 75% and 25%, respectively, in the molten carbonate fuel cell unit [22].
- Fuel utilization in the anode compartment and oxidant utilization in the cathode compartment are set at 85% and 25%, respectively, in the solid oxide fuel cell unit [24].
- All gas stream pressures are atmospheric [25].

Figure 5 shows the results of the overall energy analysis for all eight cycle configurations and Fig. 6 shows the results of overall exergy analyses for each of the eight configurations for a fixed steam-to-carbon ratio of 2.

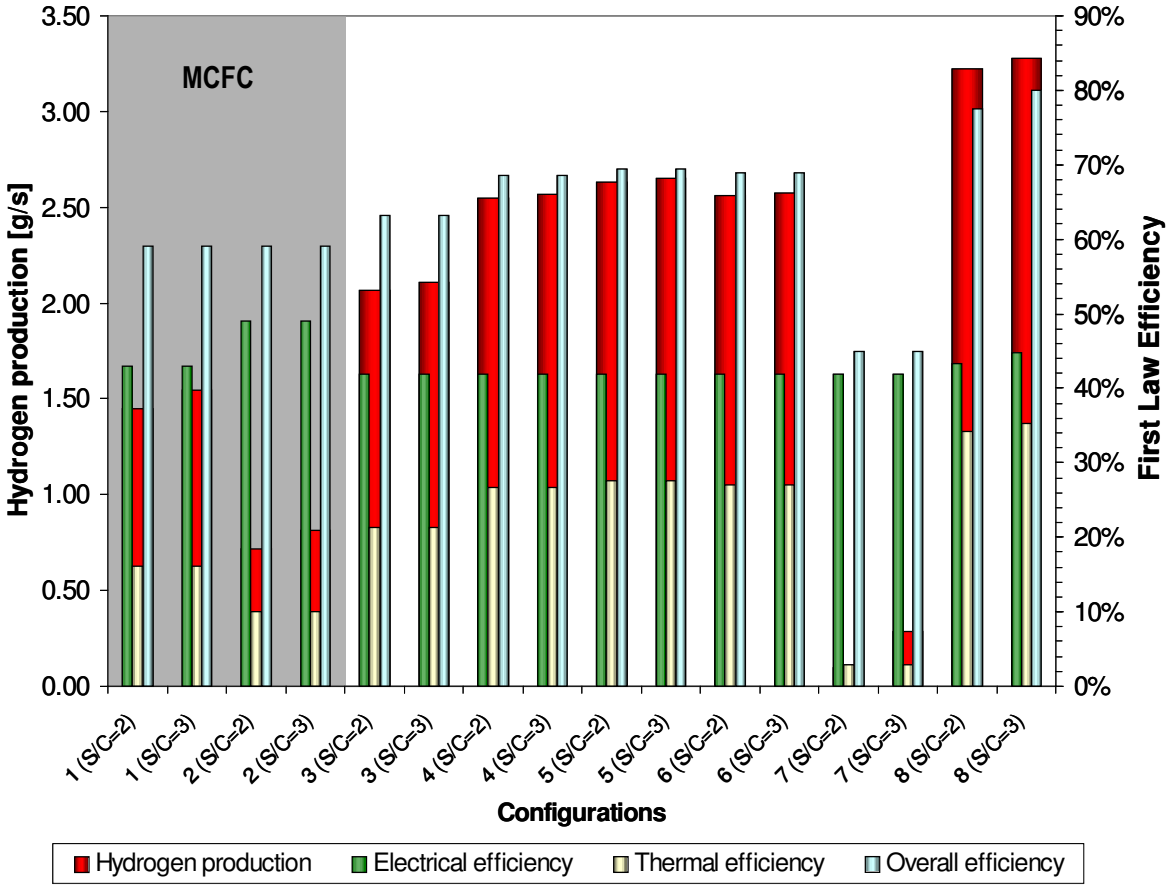

Figure 5. Results of energy performance analysis.

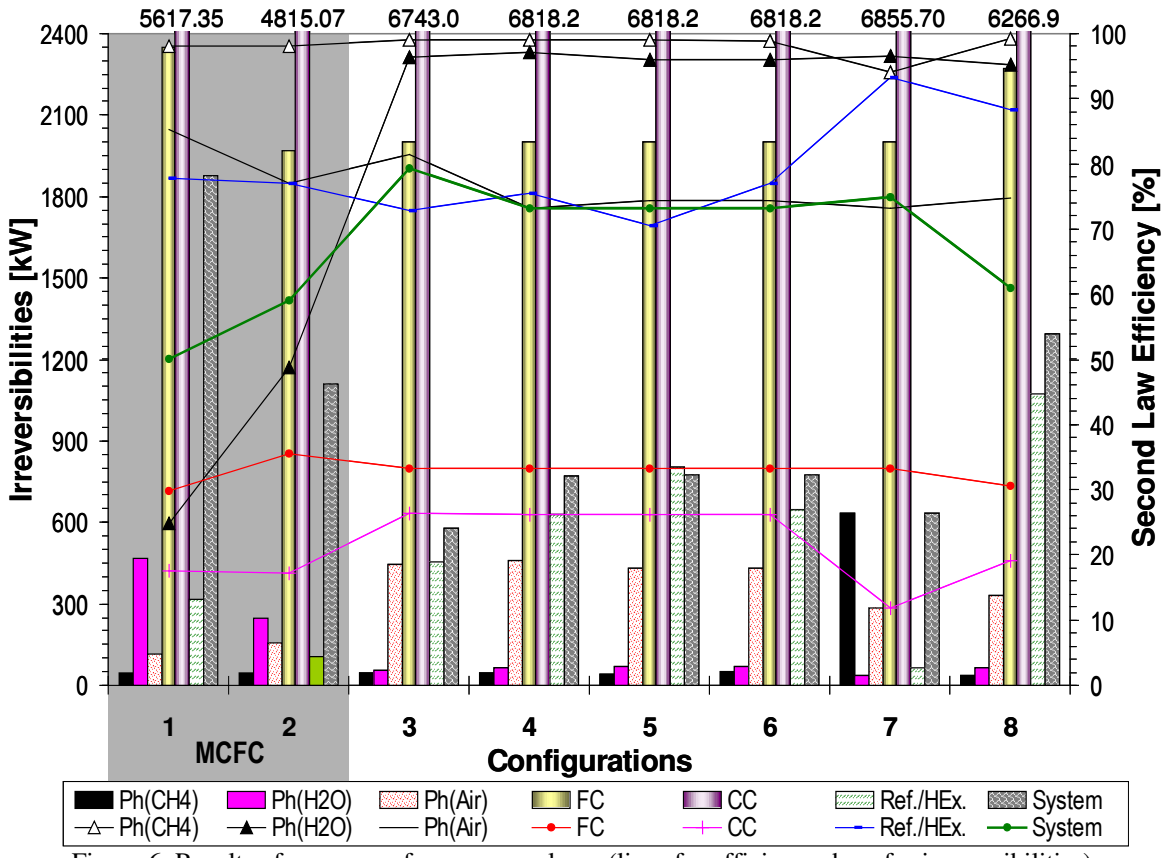

Figure 6. Results of exergy performance analyses (lines for efficiency, bars for irreversibilities).

Figure 5 shows that the overall thermodynamic efficiency of these types of integrated hydrogen and electricity producing cycles is very high. For all configurations (except #5) overall efficiencies are greater than 59%. Note that this efficiency is a "mixed" efficiency that includes electrical work and chemical energy of the hydrogen produced in the numerator. For clarity, the contributions of electricity and hydrogen energy (thermal) are each presented for all of the cases.

When comparing the energy analyses amongst cycle configurations, Figure 5 indicates that for the same amount of power produced by the fuel cell, configuration 8 (internal reforming SOFC) shows the highest potential for production of hydrogen (about 3.2 g/s for S = 2 and 3.3 g/s for S = 3) as well as the highest overall efficiency. Also, configuration 8 achieves a remarkable overall efficiency of nearly 80% for the steam-to-carbon ratio of 3. One of the reasons for this high efficiency is the synergy associated with internal reformation that is reflected in the higher electrical efficiencies for configuration 8. These higher electrical efficiencies are due to the higher exit hydrogen concentration in the fuel cell for configuration 8 leading to higher voltage potential.

Figure 5 shows that configuration 7 (combustion chamber after the air pre-heater) is the worst cycle configuration with the highest thermal losses on an energy basis. However, configuration 7 may be the most flexible configuration with regard to hydrogen production capacity (not studied in the current work). Configurations 4, 5, and 6 perform similarly with regard to hydrogen production and efficiency, but configuration 3 is slightly less efficient with lower hydrogen production capability. Also, It can be observed in Fig. 5 that the highest hydrogen production for a MCFC occurs with the configuration with uses a reformer separated from the fuel cell (external reforming) while for a SOFC the internal reforming option provided the best results.

Figure 6 presents the exergy analyses for all of the configurations, indicating the components that contribute most significantly to losses within each configuration. Components with high irreversibilities or low second law efficiency and the manner in which they are implemented in the cycle are those that designers should focus upon to improve system performance.

The exergy results of Fig. 6 show that the major destruction of exergy (irreversibility) was in the combustion chamber (CC) for all configurations. In all cases the combustion chamber is associated with the maximum temperature of the products in the integrated fuel cell system. Since the irreversibility in the combustion chamber is much larger than the other component irreversibilities the values for combustion chamber irreversibility are provided at the top of Fig. 6 for each configuration (versus plotting the irreversibility as a bar of much greater magnitude than all the others).

Several interesting results emerge from the second law analyses presented in Fig. 6. The variations in second law performance amongst the cycle configurations are primarily associated with the combustor, fuel preheater, and reformer components.

The combustor irreversibility of the internal reforming configurations (#2 and #8) is lower than those with external reforming. In the configurations 2 and 8, the product hydrogen is removed before the combustor. Hydrogen contributes to two moles of water for every mole of oxygen converted in the combustor compared to one mole for every mole of carbon converted to CO_2. Thus removal of hydrogen from the inlet stream of the combustor leads to a lower number of moles in the product stream and the lowest combustor exit exergy compared to cases with hydrogen in the inlet gases. However, inlet exergy for the internal reforming case (configurations 2 and 8) is substantially lower than those of the other cases leading to lower second law efficiency for the combustor in these configurations.

The second law efficiency for the combustor of the two MCFC configurations is similar. However, among the SOFC configurations, configuration 7 has irreversibility in the combustion chamber that is similar to configurations 3-6. The second law efficiency of the combustion chamber of configuration 7 is the lowest of all configurations due to the large temperature rise in this component placed after all of the pre-heaters. All other cases have similar second law efficiency and irreversibilities in the combustor.

In the external reforming MCFC cases, the fuel/water preheater heats up water and methane (using more fuel), which causes the values for irreversibilities to be higher than those for the internal reformation case. Also, the second law efficiency for the water preheater in the external reforming case is lower than in the internal reforming case (25% versus 48%).

For configuration 7, the fuel preheater irreversibility is higher and the second law efficiency is lower than that of all of the other configurations. This is due to the high hydrogen content of the stream entering this pre-heater for this case, since the chemical exergy of hydrogen is high compared to the water that is present in this stream for the other configurations.

Configuration 7, which shows the worst energy and hydrogen production performance, has better exergy performance in the reformer component than all the other cycle configurations because the combustor is placed immediately before the reformer leading to a better reformer operating temperature. Configuration 8 has the second highest reformer second law efficiency, which is also due to a better reformer operating temperature. The reformer of configuration 8 operates at the 1000°C temperature of the SOFC, which results in good conversion of fuel to hydrogen as indicated in Figure 5. The reformer performance of configuration 8 also benefits from concurrent electrochemical and chemical reactions in the anode compartment.

The second law efficiency (and exergy losses) in the fuel cell component is very similar in each of the cycle configurations. The difference in second law efficiency for the fuel cell configurations is slight, varying from 30% to 35%. The fuel cell irreversibility of configuration 1 is about 15% higher than configurations 2 through 7 primarily due to higher fuel throughput for the same power output. The fuel cell irreversibility difference between configurations 1 and 8 is only 3%.

The overall second law efficiency of configuration 3 is highest and configuration 1 is lowest among all the configurations considered. The second law efficiency of configuration 3 is high due to cumulative better exergy performance of the components as integrated in configuration 3. This is primarily manifested in lower irreversibilities in the fuel cell (compared to configuration 1 and 8), and the reformer (compared to all other configurations except configurations 1 and 7).

Among the SOFC configurations, configuration 8, which shows the best energy performance and hydrogen production capacity, exhibits the worst exergy performance due to a higher inlet exergy requirement. That is, more fuel is required to achieve the higher hydrogen production of configuration 8. However, what this result indicates is that there is the potential for significant performance improvements for the internal reforming option of configuration 8. These potential improvements will be addressed in future studies.

To directly compare the proposed concept to stand-alone steam reformation one final set of calculations was performed. Strict hydrogen production thermal efficiency was calculated on the basis of hydrogen energy out divided by the fraction of methane fuel input that was used to produce the hydrogen. That is, the quantity of fuel that directly produces electricity (in the fuel cell) was subtracted out of the denominator. The resulting strict hydrogen production efficiency of configurations 1 through 8, for steam-to-carbon ratio of 2.0, were 81.6%, 89.6%, 85.6%, 84.2%, 84.3%, 83.7%, 60.8%, and 85.6%, respectively. These thermal efficiency values, except for the configuration 7 value of 60.8%, are clearly superior to typical small-scale steam reformation [2] and even compete with large-scale steam methane reformation efficiencies reported in the range of 75 to 80% [2].

Further research is justified using the insight gained through the present investigation. This research should focus on those sub-processes having large exergy losses and should include, for example, process integration, design and optimization, temperature profile changes, etc.

SUMMARY AND CONCLUSIONS

The high efficiency and lower pollutant emission features of fuel cells compared to other technologies make them an attractive technology for energy generation.

This paper presents a novel method for the local co-production of hydrogen and electricity from high temperature fuel cells. Several generic cycle configurations are presented. In addition, a methodology for analyzing this concept is presented that includes thermodynamic and electrochemical analyses.

The energy analyses of various solid oxide and molten carbonate fuel cell cycles show that both fuel cell types are capable of co-producing hydrogen and electricity. The analyses further show that configurations in which the fuel is reformed inside of the fuel cell have the best energy efficiency and co-production of hydrogen capacity. Overall, the solid oxide fuel cell configuration with complete internal reformation had the highest energy efficiency and hydrogen production capacity. However, the exergy analysis of this same configuration shows that much effort should be invested to further improve this generic cycle configuration.

The electrical efficiency (ratio of the electric energy produced to the fuel thermal energy) of the systems was in the range of 41 to 49%, with the highest value for the internal reforming molten carbonate fuel cell. The overall energy efficiency (ratio of the electric energy plus hydrogen energy produced to the fuel thermal energy) ranges from 45% to 80%. The lowest overall energy efficiency was for a case that combusted fuel in the exhaust of the solid oxide fuel cell system for hydrogen production in an external reformer. The highest overall efficiency was for the internal reforming solid oxide configuration.

The hydrogen co-production concept presented in this paper is clearly worthy of further investigation, development, and demonstration. Thermodynamic analyses suggest a clear advantage of net fuel savings compared to separate generation of electricity and hydrogen, which is only augmented by the avoidance of transport energy and emissions benefits.

Fuel cell technology is advancing with several commercial products emerging into the market that may become amenable to testing the hydrogen co-production concept. But significant challenges remain, including the need for more robust high temperature fuel cells that can internally reform methane-based fuels, integration with small-scale hydrogen separation, compression and storage technology, and cost reduction.

ACKNOWLEDGMENTS

The first author would like to acknowledge CNPq (Conselho Nacional de Desenvolvimento Científico e Tecnológico, Brazil) for the financial support in this project.

REFERENCES

[1] Ahmed, S., Krumpelt, M., 2001, "Hydrogen from hydrocarbon fuels for fuel cells", International Journal of Hydrogen Energy, **26**, pp. 291–301

[2] Ogden, J.M., 2002, "Review of small stationary reformers for hydrogen production", Technical Report IEA/H2/TR-02/002, International Energy Agency

[3] Hammerli, M., 1984, "When will electrolytic hydrogen become competitive?" International Journal of Hydrogen Energy, **9** (1/2), pp. 25-51.

[4] Morse, S., 2004, "Hydrogen – The Fuel of Today" Technical report. Available at www.eng.usf.edu/rnr/ret_2004/HYDROGEN_FUEL_OF_THE_FUTURE.doc

[5] Lipman, T., 2004, "What will power the hydrogen economy?" Technical Report UCD-ITS-RR-04-10, The Natural Resources Defense Council.

[6] Appleby, A. J., 1993, Chapter 5, In: L. J. M. J. Blomen and M. N. Mugerwa (eds), Fuel Cell Systems, Plenum Press, New York.

[7] Hirschenhofer, J. H., Stauffer, D. B., Engleman, R. R., 1994, "Fuel cells: a handbook (3rd revision)". Philadelphia: Gilbert and Commonwealth, Inc., U.S. Department of Energy, contract no. DE-AC01-88FE61684.

[8] EG&G Technical Services, Inc., 2002, "Fuel Cell Handbook (sixth edition)", DOE/NETL-2002/1179, Under Contract No. DE-AM26-99FT40575, U.S. Department of Energy, Office of Fossil Energy, National Energy Technology Laboratory.

[9] Lutz, A.E., Bradshawa, R.. W., Kellera, J.O., Witmerb, D.E., 2003, "Thermodynamic analysis of hydrogen production by steam reforming", International Journal of Hydrogen Energy, **28**, pp. 159 – 167.

[10] Gordon, S., McBride, B.J., 1994, "Computer Program for the Calculation of Complex Chemical Equilibrium Compositions with Applications: I. Analysis". NASA Reference Publication 1311.

[11] Chan, S.H., Xia, Z.T., 2002, "Polarization effects in electrolyte/electrode-supported solid oxide fuel cells", Journal of Applied Electrochemistry, **32**, pp. 339–347.

[12] Chan, S.H., Khor, K.A., Xia, Z.T., 2001, "A complete polarization model of a solid oxide fuel cell and its sensitivity to the change of cell component thickness", Journal of Power Sources, **93**, pp. 130-140.

[13] Kanamura, K., Yoshioka, S., Takehara, Z., 1991, "Dependence of entropy change of single electrode on partial pressure in solid oxide fuel cell" Journal of the Electrochemical Society, **138** (7), pp. 2165-2168.

[14] Takehara, Z., Kanamura, K., Yoshioka, S., 1989, "Thermal energy generated by entropy change in solid oxide fue cell", Journal of the Electrochemical Society, **136** (9), pp. 2506-2512.

[15] Herle, J.V., Membrez, Y., Bucheli, O., 2004, "Biogas as a fuel source for SOFC co-generators", Journal of Power Sources, **127** (1-2), pp. 300-312.

[16] Yuh, C.Y., Selman, J.R., 1991, "The polarization of molten carbonate fuel cell electrodes: I. Analysis of steady state polarization data". Journal of the Electrochemical Society, **138**(12), pp. 3642 - 3648.

[17] Yuh, C.Y., Selman, J.R., 1991, "The polarization of molten carbonate fuel cell electrodes: II. Characterization by AC impedance and response to current interruption". Journal of the Electrochemical Society, **138** (12), pp. 3649 – 3655.

[18] Koh, J. H., Kang, B. S., Lim, H. C., 2001, "Analysis of temperature and pressure fields in molten carbonate fuel cell stacks". AIChe Journal, **47** (9), pp. 1941 – 1956.

[19] Utgikar, P. S., Dubey, S.P., Prasada Rao, P.J., 1995, "Thermoeconomic Analysis of Gas Turbine Cogeneration Plant - A Case Study". Journal of Power and Energy, **209**, pp. 45-54.

[20] Bedringås, K. W., Ertesvåg, I. S., Byggstøyl, S., Magnussen, B. F., 1997, "Exergy Analysis of Solid-Oxide Fuel-Cell (SOFC) Systems" *Energy*, vol. 22, pp.403-412.

[21] Leal, E. M., Silveira, J. L., 2002, Study of fuel cell cogeneration systems applied to a dairy industry. Journal of Power Sources, **106**, 102-108.

[22] Selman, J.R., 1993, Research, Development and Demonstration of Molten Carbonate Fuel Cell Systems, Fuel Cell Systems, L.J.M.J. Blomen and M. N. Mugerwa, eds., Plenum Press, New York, NY.

[23] Iwahashi, T., Yoshida, N., Kosaka, H., 1998, "High efficiency power generation from coal and wastes utilizing high temperature air combustion technology: Thermal performance of compact high temperature air preheater and MEET boiler". In: Proceedings of the International Symposium on Advanced Energy Technology. Sapporo, Japan: Hokkaido University; pp. 455 – 462.

[24] Larminie, J., Dicks, A., 2003, **Fuel Cell Systems Explained**, England: John Wiley and Sons, Inc.

[25] Dunbar, W.R.; Lior, N.; Gaggioli, R.A., 1991, "Combining fuel cells with fuel-fired power plants for improved exergy efficiency", Energy, **16** (10), pp. 1259-1274.

